Fast velocity model evaluation with synthesized wavefields

Adam Halpert

ABSTRACT

Sophisticated interpretation tools such as automatic image segmentation allow for near-instant creation of multiple, geologically-plausible velocity models for a given imaging target. However, testing each of these models via remigration of the full dataset is not computationally feasible. By using an initial image to synthesize both an areal source function and a Born-modeled dataset, a large number of models can be tested and evaluated in a fraction of the time required for even a single migration of the full dataset. Tests using synthetic 2D data suggest that this method can demonstrate the impact of imaging using different models, even with small differences among them. Furthermore, a measure of image focusing can help quantify the relative merits of the different models.

INTRODUCTION

Because of the high velocity contrast between salt and sediments, accurate interpretation of subsurface salt structures is vital to obtaining a high-quality seismic image. A variety of tools have been developed to aid interpreters in this task, including several different approaches to automatic seismic image segmentation (Lomask et al., 2007; Halpert, 2011). Methods such as these can provide several possible salt body interpretations, whether through uncertainty analysis of the boundary (Lomask, 2007) or interpreter guidance of segmentation results (Halpert et al., 2011). Because of computational constraints, it is often not feasible to run full migrations to test each of the possible models. Therefore, methods to quickly and efficiently test the imaging effects of each model are of great interest.

Several approaches to the problem of fast re-migration of seismic data have been proposed. Many of these approaches rely on a fast variant of beam migration (Hill, 1990), one form of target-oriented imaging. Beam-based methods (Wang et al., 2008) operate in the post-stack domain, and often rely on qualitative judgments of image quality to evaluate different velocity models. Pre-stack imaging methods using reverse-time migration (RTM) have also been proposed (Wang et al., 2011), and would allow for analysis of valuable velocity information in the form of subsurface-offset or angle gathers. However, at present this approach is likely only feasible when testing a small number of limited-size models. A further option, and the one explored here, is to synthesize new datasets from an initial image, and use these datasets to test

velocity models. First, a new source wavefield can be derived from the initial image using modified prestack exploding reflector modeling (Guerra, 2010). This allows information from the inevitable velocity errors in the initial model to be preserved and, hopefully, corrected. Second, a form of Born modeling (Stolt and Benson, 1986) can be used to synthesize a new dataset from the initial image (Tang and Biondi, 2010; Tang, 2011). The new dataset can be designed with an arbitrary acquisition geometry, creating opportunities for target-oriented imaging. Furthermore, since a generalized source function is used, a useful image with prestack velocity information can be obtained by migrating only a single shot. Crosstalk artifacts can be avoided by targeting only small, isolated locations from the initial image. This approach also allows for a simple quantitative measure of image quality or focusing. In the following sections, this method will be described and demonstrated using data from the 2D Sigsbee synthetic model. The accuracy and computational efficiency of the results show great promise for this method working in conjuction with automatic segmentation as part of a full 3D interactive interpretation toolbox.

METHOD

The procedure for Born modeling and migration to quickly test velocity models is detailed in Halpert and Tang (2011). To summarize, the major steps of the process are:

1. Using one or more subsurface offset gathers from the initial prestack image, create an areal source function via upward continuation. This is similar to the "exploding reflector" concept (Claerbout, 2005), but inclusion of the prestack subsurface-offset data is important for attempts to improve upon the initial velocity model. Mathematically, this areal source is described as

$$S(\mathbf{x}_s, \omega) = \sum_{\mathbf{x}'} \sum_{\mathbf{h}} G^*(\mathbf{x}' - \mathbf{h}, \mathbf{x}_s, \omega) m(\mathbf{x}', \mathbf{h}), \tag{1}$$

   where $\mathbf{x}_s = (x_s, y_s, z_s)$ are the arbitrarily defined locations where the wavefield will be recorded; $\mathbf{h}$ is the vector of subsurface half-offsets; ω is angular frequency; m is the initial image from which data is injected at isolated regions defined by $\mathbf{x}'$; and G is the Green's function propagating the wavefield to the receiver locations (here, * denotes the adjoint). Because the wavefield can be recorded at arbitrary locations, this method provides a simple means of re-datuming, which can lead to significant computational savings.

2. Use the new source function from step 1 and a reflectivity model based on the initial image to generate a new dataset with acquisition geometry best suited to image the target area. This can be accomplished via Born modeling, if we synthesize the new dataset d' and record it at arbitrary receiver locations $\mathbf{x}_r$:

$$d'(\mathbf{x}_r, \omega) = \sum_{\mathbf{x}'} \sum_{\mathbf{h}} \Gamma(\mathbf{x}_s, \mathbf{h}, \omega) G(\mathbf{x}' + \mathbf{h}, \mathbf{x}'_r, \omega) m(\mathbf{x}', \mathbf{h}). \tag{2}$$

Here, m is the reflectivity model (in our case, the isolated regions from the initial image), and the Γ term is defined as

$$\Gamma(\mathbf{x}_s, \mathbf{h}, \omega) = \sum_{\mathbf{x}_s} S(\mathbf{x}_s, \omega) G(\mathbf{x}_s, \mathbf{x}' - \mathbf{h}, \omega), \tag{3}$$

where S is the source function described in step 1. Because the velocity model used to compute the Green's functions is the same one used to generate the initial image, the resulting Born-modeled wavefield $d'(\mathbf{x}'_r, \omega)$ will be kinematically invariant regardless of the initial model (Tang, 2011). This is important because the initial model will inevitably contain errors, and the goal of the procedure described here is to improve upon it.

3. Using the synthesized data obtained in Step 2, and the source function from Step 1, generate an image using standard downward-continuation migration:

$$m'(\mathbf{x}', \mathbf{h}) = \sum_{\omega} G^*(\mathbf{x}' - \mathbf{h}, \omega) \sum_{\mathbf{x}_r} G^*(\mathbf{x}' + \mathbf{h}, \mathbf{x}'_r, \omega) d'(\mathbf{x}_r, \omega). \tag{4}$$

Now, *any* velocity model can be used to compute the Green's functions. This step is extremely computationally efficient compared to a full migration of the original data, allowing for testing of several possible velocity models in a fraction of the time it would take to evaluate them using standard migration techniques.

With the procedure outlined above, significant savings may be realized if only a single shot is migrated, a situation made possible by the fact that an areal source function is used along with an arbitrary acquisition geometry. However, in many cases an image obtained in this manner is contaminated by crosstalk artifacts. Various solutions to the crosstalk attenuation problem have been proposed, for example using multiple phase-encoded shots (Romero et al., 2000; Tang, 2008). Unfortunately, this approach would hinder the computational efficiency of the evaluation procedure – one of its primary considerations. Instead, the procedure described above is applied only to isolated locations from a single reflector in the initial image. As long as these locations are separated by at least twice the maximum subsurface offset value used to synthesize the new source and receiver wavefields, any crosstalk problems should be avoided. This method also allows an interpreter or model-builder to select reflectors he or she thinks would be most sensitive to changes in the velocity model – for example, the base of salt.

Evaluation criteria

Since the goal of the steps outlined above is to test the accuracy of several different models, there must be a way to judge or evaluate the images corresponding to each. In some cases, a qualitative judgment may suffice; for example, if one model clearly focuses the data at zero subsurface-offset. However, a quantitative measure of image

quality would also be useful. Since only isolated locations are being imaged, we can expect a "perfect" velocity model to focus all an image's energy at zero subsurface-offset. Therefore, a simple measure of image quality calculates what proportion of the energy indeed resides at zero or near-zero subsurface-offset:

$$F = \frac{\sum_{i=\mathbf{p}} |A_i|}{\sum_{i=\mathbf{p}} |A_i| \exp\left(\alpha \frac{|h_i|}{h_{\max}}\right)}, \tag{5}$$

where $\mathbf{p}$ is the set of all image points, A_i is the amplitude at a given point, h_i is the subsurface offset at that point, and α is an optional user-specified weighting parameter. This idea is similar to the motivation behind some inversion schemes such as differential semblance optimization (Symes and Carazzone, 1991). Using this measure, a value of $F = 1$ means that all energy is perfectly focused at zero offset; as F decreases toward zero the image becomes progressively less focused. Ideally, a measure such as this one would allow a more rigorous comparison among possible models when a more qualitative comparison fails to yield an obvious result.

SYNTHETIC EXAMPLE

The above procedure will now be demonstrated using two different initial images derived from the Sigsbee synthetic model. Figure 1(a) is a perfect-velocity, full migration of the Sigsbee data, which will be used for the first example. Figure 1(b) shows a manually-picked reflector chosen for further analysis; in this case, the base salt has been chosen because it should be particularly sensitive to different interpretations of the salt body's shape and velocity, the two model variations that will be tested. Finally, Figure 2 shows two image locations isolated from the selected reflector. Note that most of the energy is focused near zero subsurface-offset, since the true velocity model was used for the initial image.

After synthesizing the source and receiver wavefields as described in the previous section, the new wavefields were imaged using three different velocity models. First, the true model, seen in Figure 3(a). Second, an alternative model created via automatic image segmentation, in which an interpreter has chosen to include an extra chunk of salt (Figure 3(b)). The third model tested was identical to the true model in salt shape, but with a salt velocity 5% slower than the true model.

Resulting images from the Born-modeled data are seen in Figure 4. Panel 4(b), the result of migrating with the extra-salt model in Figure 3(b), is clearly the least well-focused image. However, it is difficult to qualitatively distinguish between the other two results. Table 1 gives the results of calculating the F value from equation 5 for each of the images. As expected, the result using the true model has a higher F value, indicating it is more well-focused.

The second example uses an initial image created with an incorrect velocity model; in this case, the "slow salt" model described above. The results corresponding to each

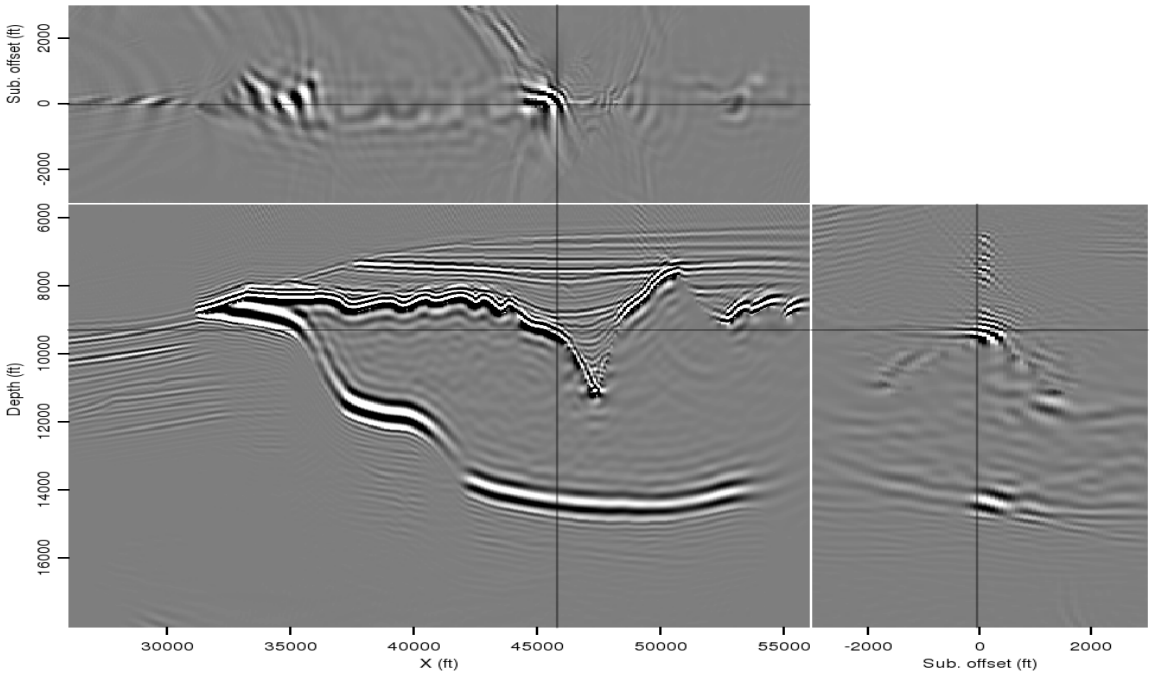

(a)

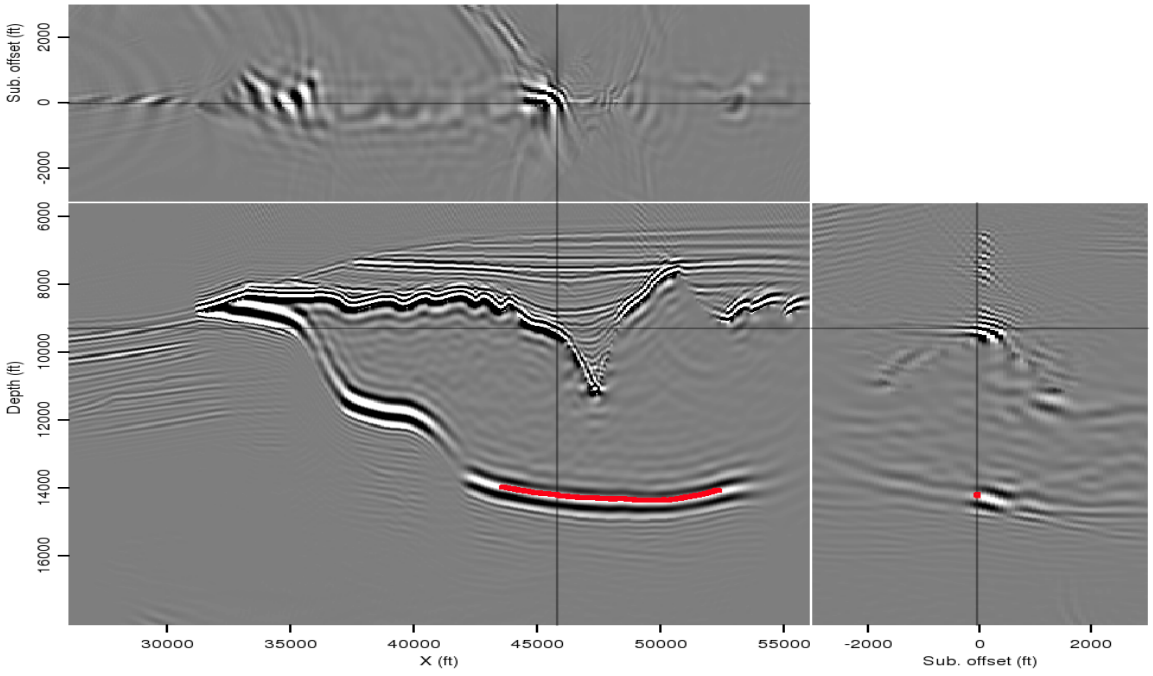

(b)

Figure 1: (a) A true velocity image using data from a section of the Sigsbee synthetic model; and (b) a base-of-salt reflector selected for further analysis because of its sensitivity to changes in the salt interpretation. [**CR**]

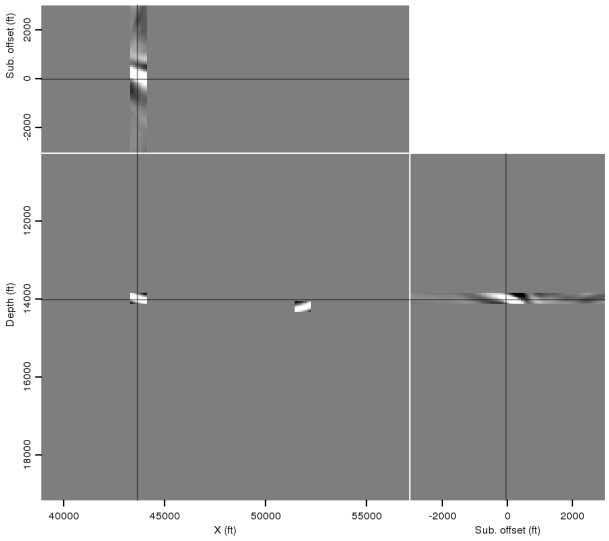

Figure 2: Isolated image locations selected from the reflector picked in Figure 1(b). [**ER**]

Migration model	F value
True velocity	0.883
Extra salt	0.879
Slow salt	0.864

Table 1: Calculations from equation 5 for each migration velocity model, after the initial image and synthesized wavefields were created using the true velocity model.

velocity model can be seen in Figure 5. Again, the extra-salt model is clearly inferior, but the differences between the other two results are more subtle. The F-value calculations in Table 2 confirm that the true model yields the optimal result, even though the slow-salt model was used to create the initial image and both synthesized datasets. In both examples, the differences between the calculated F values are relatively small; further investigation should determine how confidently such differences may be interpreted, especially when working with noisier field data.

Migration model	F value
True velocity	0.621
Extra salt	0.561
Slow salt	0.613

Table 2: Calculations from equation 5 for each migration velocity model, after the initial image and synthesized wavefields were created using the "slow salt" velocity model.

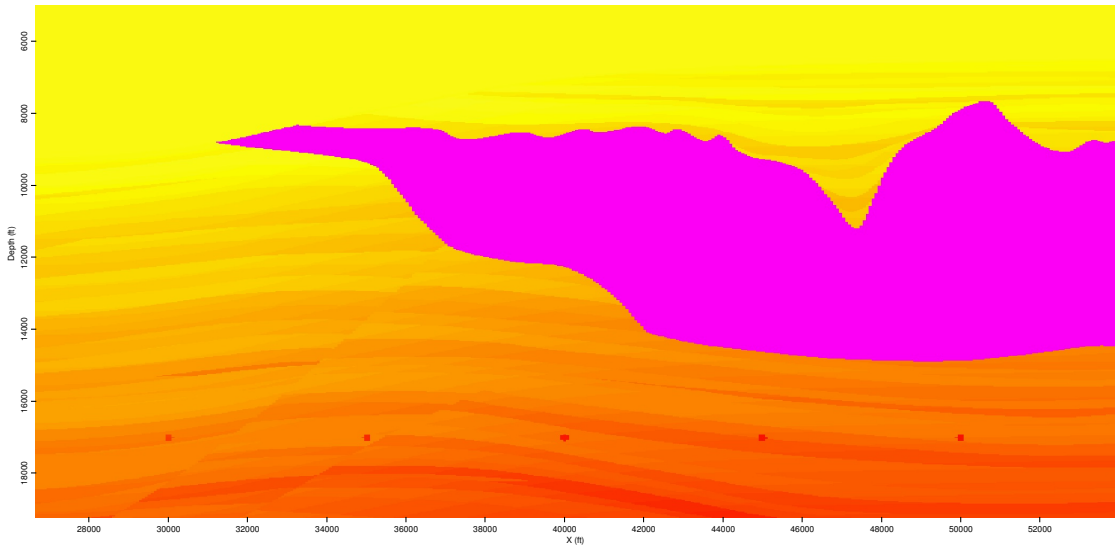

(a)

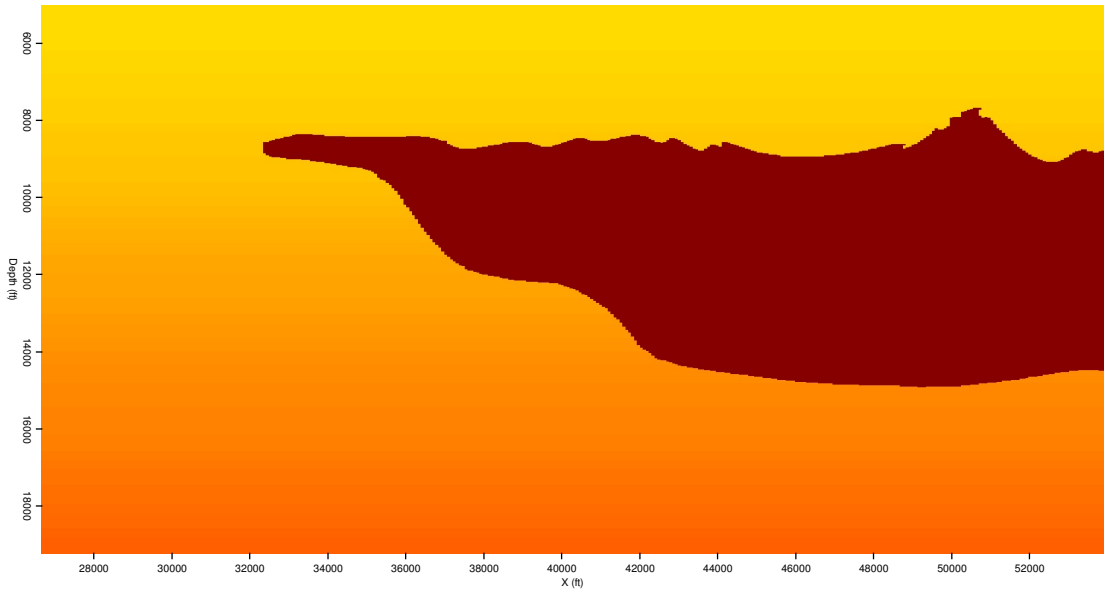

(b)

Figure 3: Two different velocity models to be tested. The model in (a) is the true Sigsbee model, while (b) is an alternate model created by one possible automatic segmentation of the initial image. [**ER**]

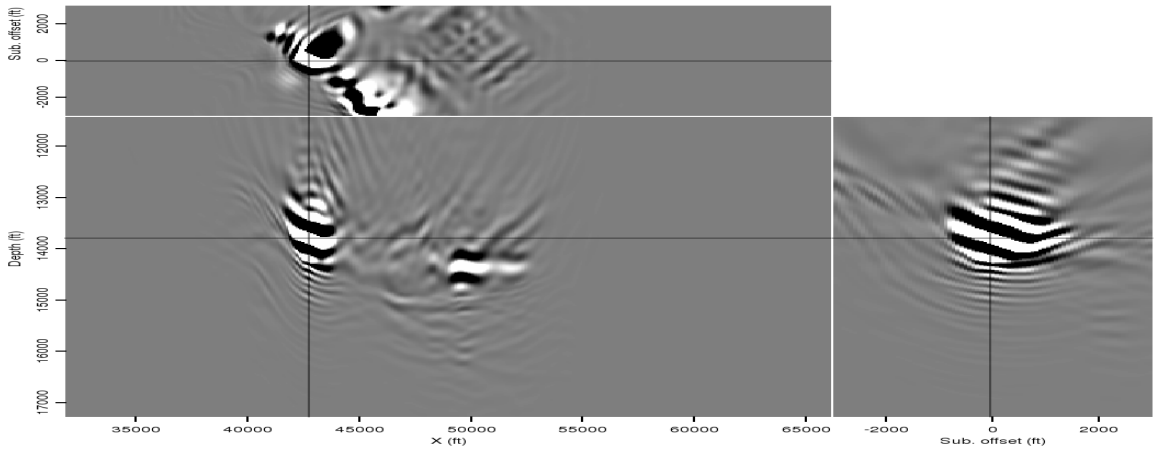

(a)

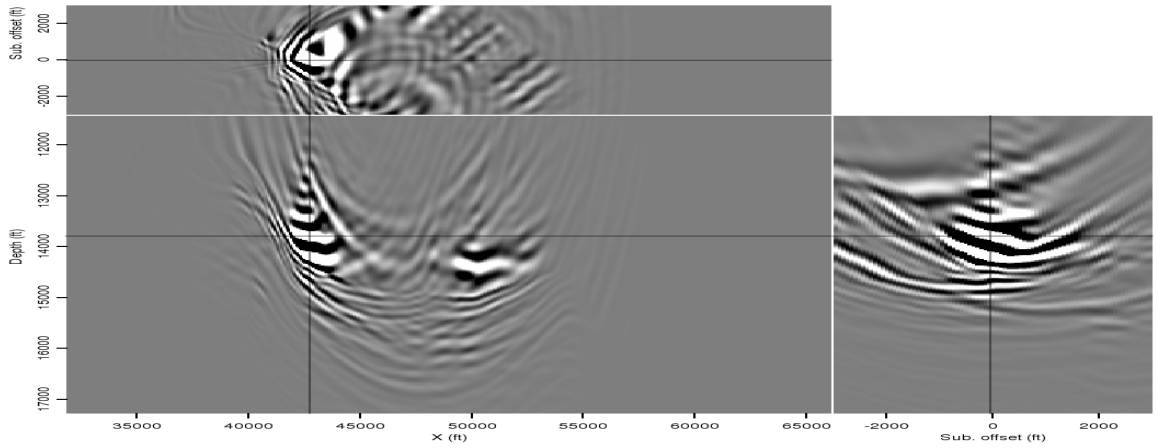

(b)

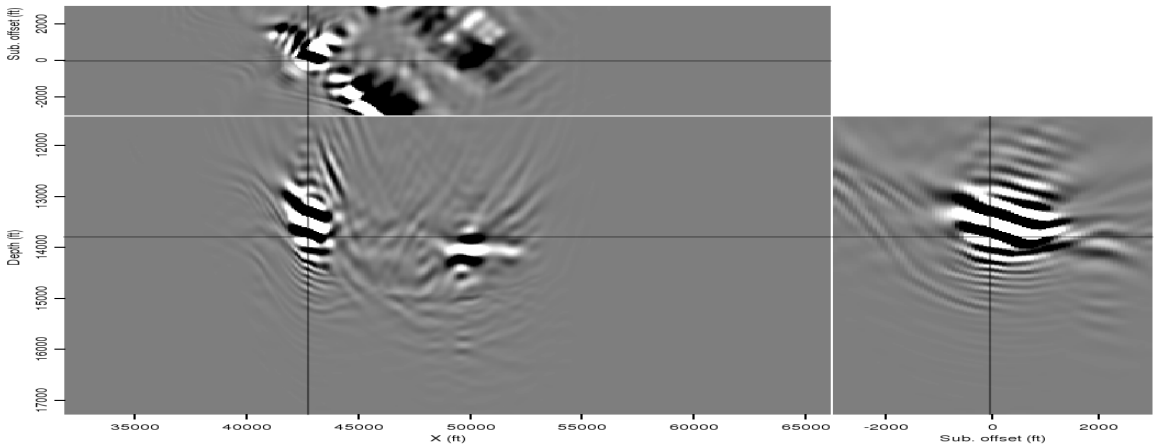

(c)

Figure 4: Three images of the Born-modeled data using three different migration velocity models: (a) the true model; (b) the extra-salt model; and (c) the slow-salt model. In this example, the initial image was created with the true model. [**ER**]

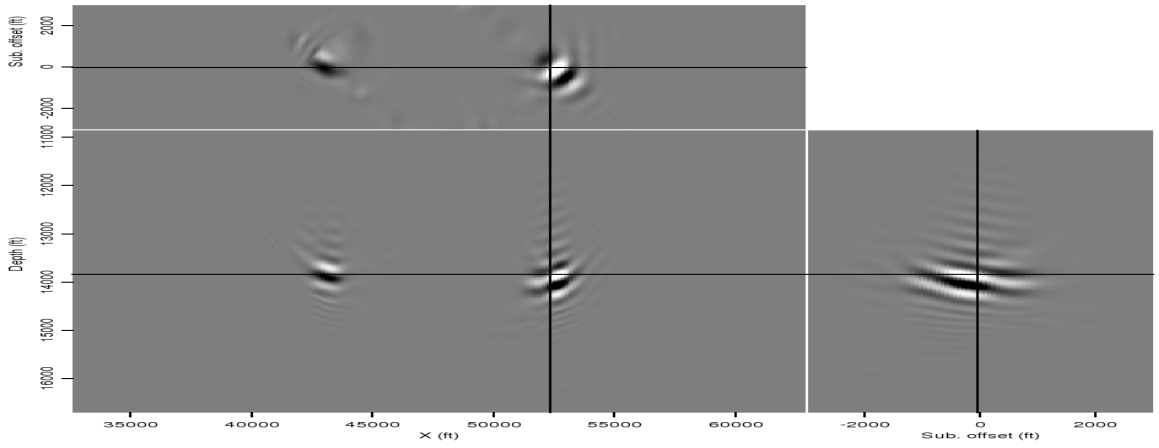

(a)

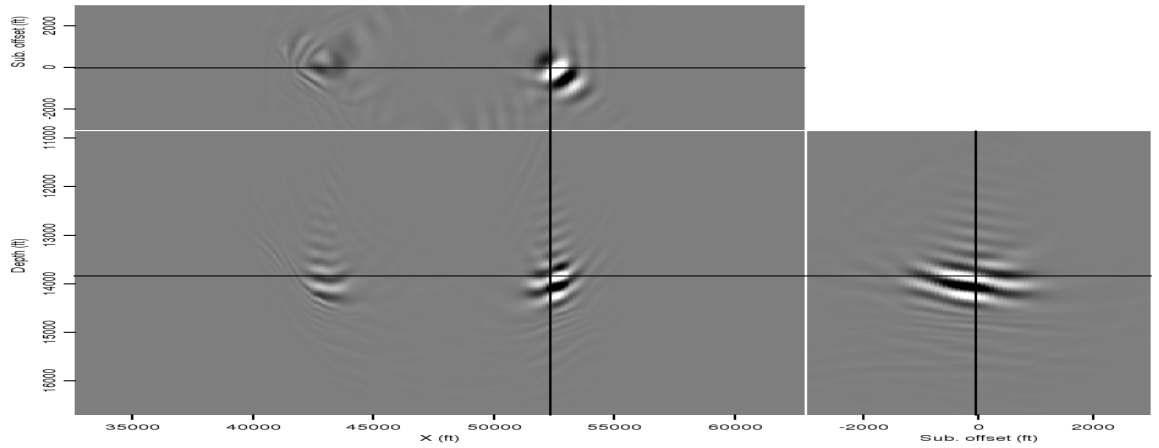

(b)

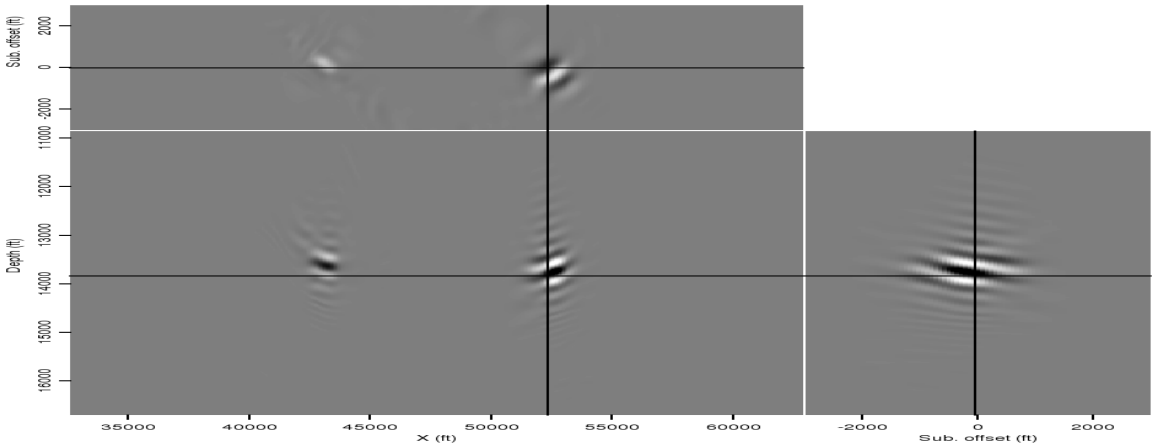

(c)

Figure 5: Three images of the Born-modeled data using three different migration velocity models: (a) the true model; (b) the extra-salt model; and (c) the slow-salt model. In this example, the initial image was created with the slow-salt model. [**ER**]

CONCLUSIONS

When several different velocity models are options for a given dataset, they can be quickly tested using wavefields synthesized from an initial image. Incorporating prestack velocity information from the initial image into both an areal source function and a Born-modeled receiver wavefield allows errors in the initial model to be taken into account and rectified when a more accurate model is tested. Finally, by imaging only isolated locations along a reflector, tests can be conducted in a fraction of the time required for a full migration by migrating only a single shot. Tests on data from the Sigsbee synthetic model demonstrated that this method can effectively discriminate between models, even if they differ only slightly in terms of salt shape or velocity, or if the initial image was created with an inaccurate model. Finally, a quantitative measure of image quality helped identify the most accurate model when qualitative comparisons were inconclusive.

ACKNOWLEDGMENTS

I thank SMAART JV for providing the Sigsbee synthetic model used for examples, and Yaxun Tang for his work on the Born modeling/migration framework used extensively here.

REFERENCES

Claerbout, J., 2005, Basic earth imaging: Stanford University.

Guerra, C., 2010, Migration-velocity analysis using image-space generalized wavefields: PhD thesis, Stanford University.

Halpert, A., 2011, Interpreter input for seismic image segmentation: SEP-Report, **143**, 237–248.

Halpert, A. and Y. Tang, 2011, Velocity model evaluation through Born modeling and migration: a feasibility study: SEP-Report, **145**, 15–26.

Halpert, A. D., R. G. Clapp, and B. L. Biondi, 2011, Interpreter guidance for automated seismic image segmentation: 74th EAGE Conference and Exhibition.

Hill, N. R., 1990, Gaussian beam migration: Geophysics, **55**, 1416–1428.

Lomask, J., 2007, Seismic volumetric flattening and segmentation: PhD thesis, Stanford University.

Lomask, J., R. G. Clapp, and B. Biondi, 2007, Application of image segmentation to tracking 3D salt boundaries: Geophysics, **72**, P47–P56.

Romero, L. A., D. C. Ghiglia, C. C. Ober, and S. A. Morton, 2000, Phase encoding of shot records in prestack migration: Geophysics, **65**, 426–436.

Stolt, R. H. and A. Benson, 1986, Seismic migration: Theory and practice: Geophysical Press.

Symes, W. W. and J. J. Carazzone, 1991, Velocity inversion by differential semblance optimization: Geophysics, **56**, 654–663.

Tang, Y., 2008, Modeling, migration, and inversion in the generalized source and receiver domain: SEP-Report, **136**, 97–112.

———, 2011, Imaging and velocity analysis by target-oriented wavefield inversion: PhD thesis, Stanford University.

Tang, Y. and B. Biondi, 2010, Target-oriented wavefield tomography using demigrated Born data: SEP-Report, **140**, 67–82.

Wang, B., J. Ji, C. Mason, S. Gajawada, and Y. Kim, 2008, Beam-based interactive imaging for salt interpretation and salt model building: SEG Technical Program Expanded Abstracts, **27**, 3073–3077.

Wang, B., C. Mason, K. Yoon, J. Ji, J. Cai, S. Suh, and Z. Li, 2011, Complex salt model building using a combination of interactive imaging and layer-stripping RTM: First Break, **29**, 47–54.